AMERICAN ACADEMY OF OPHTHALMOLOGY®

A Novel Time-Aware Deep Learning Model Predicting Myopia in Children and Adolescents

Ana Maria Varošanec, MD,[1,2] *Leon Marković, MD,*[1,2] *Zdenko Sonicki, MD, PhD*[3]

Objective: To quantitatively predict children's and adolescents' spherical equivalent (SE) by leveraging their variable-length historical vision records.

Design: Retrospective analysis.

Participants: Eight hundred ninety-five myopic children and adolescents aged 4 to 18 years, with a complete ophthalmic examination and retinoscopy in cycloplegia prior to spectacle correction, were enrolled in the period from January 1, 2008 to July 1, 2023 at the University Hospital "Sveti Duh," Zagreb, Croatia.

Methods: A novel modification of time-aware long short-term memory (LSTM) was used to quantitatively predict children's and adolescents' SE within 7 years after diagnosis.

Main Outcome Measures: The utilization of extended gate time-aware LSTM involved capturing temporal features within irregularly sampled time series data. This approach aligned more closely with the characteristics of fact-based data, increasing its applicability and contributing to the early identification of myopia progression.

Results: The testing set exhibited a mean absolute prediction error (MAE) of 0.10 ± 0.15 diopter (D) for SE. Lower MAE values were associated with longer sequence lengths, shorter prediction durations, older age groups, and low myopia, while higher MAE values were observed with shorter sequence lengths, longer prediction durations, younger age groups, and in premyopic or high myopic individuals, ranging from as low as 0.03 ± 0.04 D to as high as 0.45 ± 0.24 D.

Conclusions: Extended gate time-aware LSTM capturing temporal features in irregularly sampled time series data can be used to quantitatively predict children's and adolescents' SE within 7 years with an overall error of 0.10 ± 0.15 D. This value is substantially lower than the threshold for prediction to be considered clinically acceptable, such as a criterion of 0.75 D.

Financial Disclosure(s): The author(s) have no proprietary or commercial interest in any materials discussed in this article. *Ophthalmology Science 2024;4:100563 © 2024 by the American Academy of Ophthalmology. This is an open access article under the CC BY-NC-ND license (http://creativecommons.org/licenses/by-nc-nd/4.0/).*

Myopia stands as one of the most prevalent refractive errors of the eye, affecting a substantial proportion of the global population. It is estimated that the prevalence of myopia will be >50% by 2050.[1] Currently, the management and therapy of myopia aim to slow down its progression and minimize its impact on vision.[2] Spectacles are the prevailing choice for correcting myopia, with an extensive range of newly developed contact lenses and spectacles demonstrating notable effectiveness in impeding its progression.[3] Additionally, widely adopted and effective methods for myopia control encompass the usage of low-dose atropine eye drops and orthokeratology.[3–5] To identify high risk children and adolescents for more timely and effective intervention, in recent years, research has increasingly focused on predicting myopia onset and progression, considering various factors such as genetics, sex, age, environmental influences, initial refractive error, and corneal shape and structure et cetera.[6–9] Collecting large-scale fact-based clinical data that are unified and reliable is a slow and prolonged process, and for this reason historical demographic and refractive data depicting myopia progression can be associated with future changes in visual acuity.[10]

Utilization of big databases provides sample data for training and refining predictive models, enhancing their accuracy and robustness in making informed predictions.[11] Understanding data and objectives, data cleaning and preparation, exploratory data analysis, machine learning, and predictive models are critical steps in effectively analyzing a large database and extracting valuable insights to support decision-making and achieving analytical objectives like variable predictions.[12] Analysis of big databases engaging deep learning excels at understanding complex nonlinear parameters and data structures. It often outperforms traditional models in medical prediction tasks.[13–15] Nevertheless, applications of deep learning in predicting myopia are quite limited.

Since refractive eye examination data consists of irregular and asynchronous time series data, Liu et al presented an advanced machine learning technique capturing temporal features in such samples, called knowledge guided

https://doi.org/10.1016/j.xops.2024.100563
ISSN 2666-9145/24

time-aware long short-term memory (T-LSTM).[16] Considering the structure of our data, we incorporated 2 time-aware gates that adjust the memory content according to the elapsed time since the last visit and the elapsed time since the last measured values for all variable streams, predicting children's and adolescents' spherical equivalent (SE) based on their variable-length historical vision records up to 7 years after first examination.

Methods

Data Description

The dataset utilized in this study comprises 46 643 historical vision records from 13 364 children and adolescents aged 4 to 18 years diagnosed with refractive error and followed-up at the pediatric ophthalmology clinics of the University Eye Department of University Hospital "Sveti Duh" within the period from January 1, 2008 to July 1, 2023 in Zagreb, Croatia. Patients were subjected to a standardized assessment of visual acuity using a logarithmic visual acuity logarithm of the minimum angle of resolution inline chart. The assessments were conducted at both near (40 cm) and distance (3 m) settings, with evaluations performed monocularly and binocularly. These evaluations were carried out with and without correction, encompassing diopters (D) of spheres and cylinders on specific axis degrees. The study included the assessment of both uncorrected visual acuity and best-corrected visual acuity. These measurements were obtained using subjective refraction, and visual acuity was determined through retinoscopy in cycloplegia. Tropicamide 1% (sold as Mydriacyl by Alcon Laboratories Inc) was administered into each eye of the patient in a series of 3 applications, spaced 15 minutes apart. This protocol aimed to attain optimal mydriasis and cycloplegia for the examination. A complete ophthalmic assessment was conducted, encompassing both slit lamp examination and indirect fundus examination. The purpose was to rule out any ocular comorbidities and potential underlying factors contributing to myopia. Additionally, comprehensive data were gathered, including self-reported medical history and input from legal guardians. This encompassed details about prior ophthalmic conditions, surgeries, and any instances of myopia within the family. All this information was documented for further analysis. Ophthalmic examinations were conducted by experienced pediatric ophthalmologists.

Inclusion criteria: children and adolescents from Central and Southeastern Europe, aged $\geq$4 and $<$19 years, diagnosed with primary myopia or compound myopic astigmatism with a minimum of 2 visits, in addition to the first and last visit spaced by no $<$6 months apart. Exclusion criteria: patients with eye comorbidities, including mixed astigmatism, strabismus, corneal diseases, retinopathy of prematurity, amblyopia, patients $\geq$19 years of age, and patients allergic to cycloplegic drugs.

Adhering to the International Myopia Institute definition,[17] premyopia was characterized as a state where the SE refractive error of an eye falls within the range of >-0.50 D and $\leq$0.75 D when ocular accommodation is at rest. Low myopia was classified as a condition where the SE refractive error of an eye is ≤-0.50 D and >-6.00 D when ocular accommodation is relaxed. High myopia was identified as a condition in which the SE refractive error of an eye is ≤-6.00 D when ocular accommodation is relaxed.

Spherical equivalent was calculated as spherical power plus half of the cylindrical power.

The dataset consisted of electronic medical records representing initial and follow-up visits, each containing 16 distinct features.

The features included unique identifiers for each individual, date of first and follow-up visits (check date), demographic factors (school-age group, gender, and age), refractive characteristics (correction method, uncorrected visual acuity, best-corrected visual acuity, best-corrected visual acuity binocularly, baseline cycloplegic SE, corrected SE, sphere, cylinder, and axis), parental myopia status, and myopia classification. Table 1 presents baseline statistics for both discrete and continuous variables, while Figure 1 and 2 visualize their respective distributions.

Data Preprocessing

To mitigate any potential interference stemming from the original sequential encoding of categorical features, such as correction method and gender, we applied one-hot encoding. This technique creates unit vectors representing each distinct option within a categorical feature. The dimensionality of each vector corresponds to the total number of categories within the feature.[18] For instance, considering parental myopia as a categorical feature, a possible one-hot encoding could represent both myopic parents as (1, 0, 0), 1 myopic parent as (0, 1, 0), and nonmyopic parent as (0, 0, 1).

Following the process of one-hot encoding, features were standardized except for "ID," which functions as a unique identifier specific to each individual in the dataset, and "check date," reflecting the date of the examination, to expedite model convergence. The standardization rescales the sample mean to zero ($\mu = 0$) and variance to unit ($\sigma = 1$),[19] as

$$x' = \frac{x - \mu}{\sigma}$$

In order to augment the sample size, the historical records of each child or adolescent were divided into multiple samples. It was ensured that all input data utilized for training and prediction was recorded prior to the corresponding label (i.e., the SE value). For example, an idividuals's 3 records (a, b, c) belonging can be divided into 4 distinct samples, each predicting subsequent records within defined time intervals:

1. Record [a] predicts record [b] SE, over time interval [ab].
2. Record [a] predicts record [c] SE, over time interval [ac].
3. Record [b] predicts record [c] SE, over time interval [bc].
4. Records [a] and [b] predict record [c] SE, over the time intervals [ab] and [bc].

The dataset was then segmented into layers based on sequence lengths. Subsequently, each layer was partitioned into a training set (80%), a validation set (10%), and a testing set (10%).

Extended Gate Time-Aware Long Short-Term Memory

The recurrent neural network (RNN) architecture is proficient in capturing long-term memory by effectively incorporating contextual information. However, it grapples with the challenge of gradient vanishing or exploding, which impacts its training and learning process.[20,21]

To overcome this challenge, long short-term memory (LSTM)[22] integrates short-term and long-term memory via gate control mechanisms. However, it operates under the assumption that the time intervals between sequential elements are uniformly distributed, thus limiting its ability to handle irregular time intervals.

Introducing time-aware LSTM, it implements time interval information based on the standard LSTM, attenuating short-term

Table 1. Study Group Baseline Feature Description

Features	Statistics
School-age group	Preschool (140), elementary school (1st−4th grade) (273), elementary school (5th−8th grade) (360), high school (122)
Gender	Male (371), female (524)
Age (yrs)	11.20 ± 3.56 [4.09, 18.95] (895)
Correction method	Uncorrected (190), spectacles, glasses (1600)
UCVA (decimal)	0.71 ± 0.19, [0.2, 1] (1790)
Sphere (D)	−1.79 ± 1.55, [−12.50, 0.25] (1790)
Cylinder (D)	−0.61 ± 0.72, [−5.00, 0.75] (1790)
Axis (°)	With-the-rule astigmatism (1056), against-the-rule astigmatism (208), 3 oblique astigmatism, [0, 180] (40)
BCVA (decimal)	0.96 ± 0.09, [0.4, 1] (1790)
BCVA binocularly (decimal)	0.99 ± 0.04, [0.4, 1] (895)
Parental myopia	Nonmyopic parents (514), 1 myopic parent (310), both parents myopic (71)
Myopia classification	Premyopia (51), low myopia (813), high myopia (31)
Baseline cycloplegic SE (D)	−1.94 ± 1.63, [−11.87, 0.00] (1790)
Corrected SE (D)	−1.60 ± 1.56, [−11.87, 0.00] (1790)

Discrete variables: distinct category (N).
Continuous variables: mean ± standard deviation, [min, max] (N). Axis values follow a bimodal distribution, so the mean value and standard deviation are less meaningful. Therefore, we treat it as a quasi-categorical variable with 3 classes: with-the-rule astigmatism ($60° \leq$ Axis $\leq 120°$), against-the-rule astigmatism (Axis $< 30°$ or Axis $> 150°$), and oblique astigmatism ($30° \leq$ Axis $< 60°$ or $120° <$ Axis $\leq 150°$). Detailed distribution is shown in Figures 1 and 2.
BCVA = best-corrected visual acuity; D = diopters; SE = spherical equivalent; UCVA = uncorrected visual acuity.

memory according to the time intervals in order to capture the temporal dynamics of the sequential data with temporal irregularity.[23] Time-aware LSTM distinguishes itself from the standard LSTM primarily through its modification of short-term memory, which is tailored based on the time intervals between records during the subspace decomposition of the previous time step. The issue arises during the import of incomplete data. In cases where an individual is content with their current spectacle correction, not all historical data for that particular individual will consistently contain retinoscopy under cycloplegia. To bypass loss of data and complement the time-series datasets, adjustment of short-term memory to not only time intervals between variable streams was

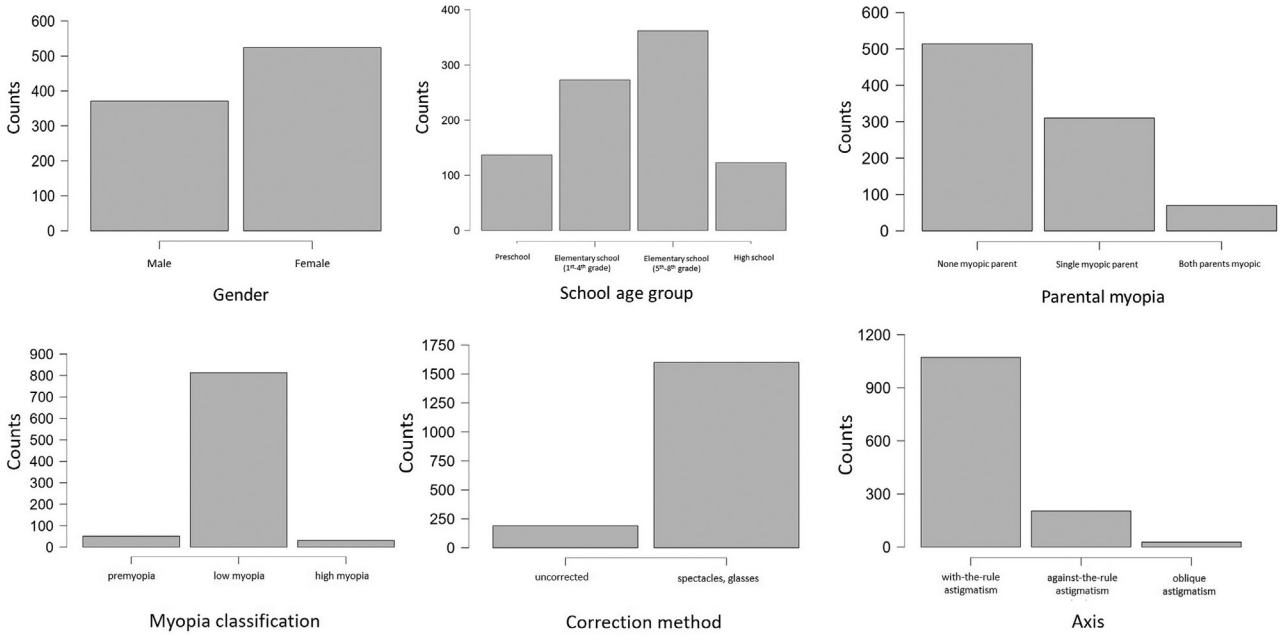

Figure 1. Baseline distributions of discrete features. School age group, gender, myopia classification, and parental myopia count was related to number of individuals (N = 895). Correction method and axis was counted for each eye (N = 1790).

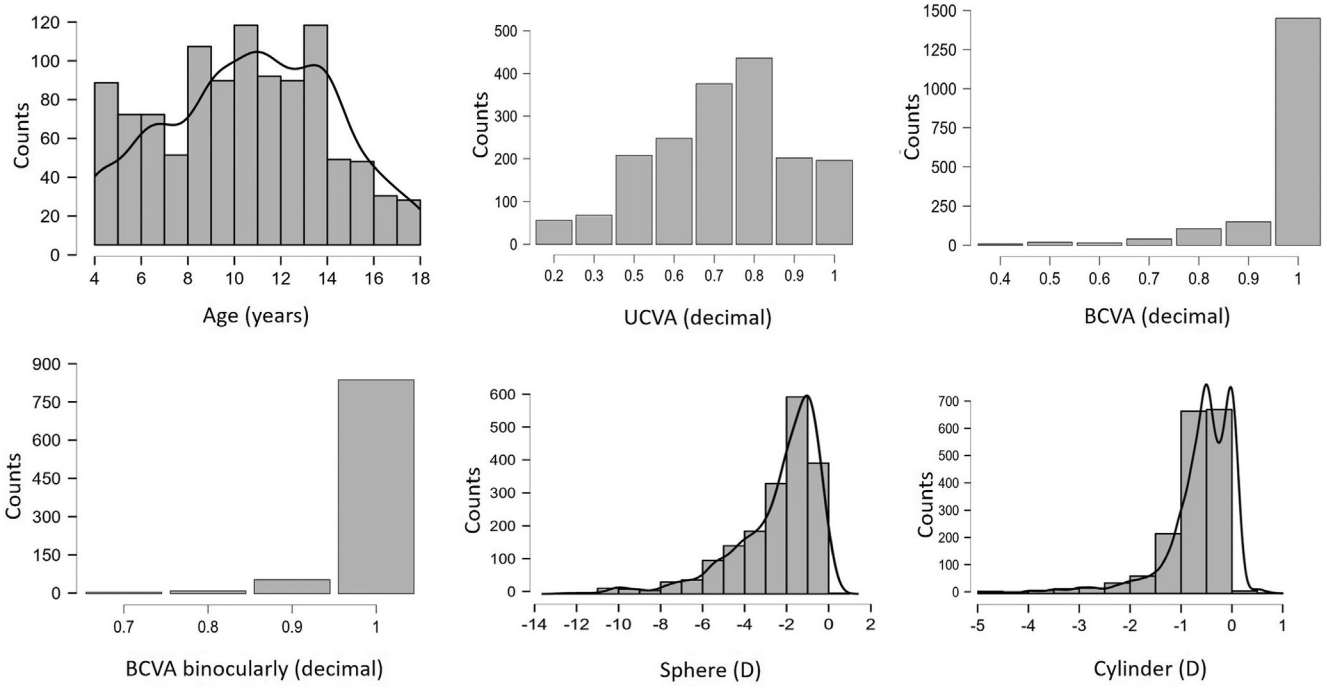

Figure 2. Baseline distributions of continuous features. Age was related to number of individuals (N = 895). Uncorrected visual acuity, BCVA, best corrected binocular visual acuity (BCVA binocularly), sphere, and cylinder was counted for each eye (N = 1790). BCVA = best corrected distance visual acuity; D = diopter; UCVA = uncorrected distance visual acuity.

accomplished, but additionally, the elapsed time since the last measured values for each variable stream was incorporated, proposing extended gate time-aware LSTM (egT-LSTM).

Extended gate time-aware LSTM unit features a forget gate, an input gate, an output gate, and a cell state. The current state h_t is influenced by the previous state h_{t-1} and the current input x_t.

Forget gate:[24]

$$f_t = \sigma\left(W_f\, x_t + U_f\, h_{t-1} + b_f\right)$$

Input gate:[25,26]

$$i_t = \sigma\left(W_i x_t + U_i h_{t-1} + b_i\right)$$

$$\tilde{C}_t = tanh(W_c x_t + U_c h_{t-1} + b_c)$$

Output gate:[27,28]

$$o_t = \sigma\left(W_o x_t + U_o h_{t-1} + b_o\right)$$

$$ht = o_t \cdot tanh\left(C_t\right)$$

Cell state:[29]

$$C_t = f_t \cdot C*_{t-1} + i_t \cdot \tilde{C}_t$$

where σ and tanh represent the activation functions, W, U, and b are the learnable parameters, and · is the Hadamard product.

Extended gate time-aware LSTM extends LSTM with 2 time-aware gates. The short-term time-aware gate g_t is updated by the elapsed time since the last time step, and the long-term time-aware gate g_t' is updated by the elapsed time since last measured value for each feature.[30,31]

$$g_t = \sigma(1 / \Delta_t)$$

$$g_t' = \sigma\left(W_g(1 / \sigma(\Delta_t')) + b_g\right)$$

Based on the description provided in T-LSTM,[23] we isolated both the short-term and long-term memory components from the preceding memory cell C_{t-1}, denoted as C^S_{t-1} and C^L_{t-1}. Subsequently, we modified the short-term and long-term memory independently using their respective time-aware gates g_t and g_t'. More specifically, the short-term memory undergoes a discounting process based on the time that has passed since the last time step, while the long-term memory is discounted based on the time elapsed since the last recorded values. We labeled the discounted short-term and long-term memory cell as C^{DS}_{t-1} and C^{DL}_{t-1}. Lastly, the aggregate adjusted prior memory cell, denoted as C^*_{t-1}, is calculated by summing the discounted short-term and long-term memories. The computation for memory cells is expressed as[22,23,32–34]:

$$C^S_{t-1} = \tanh(W_d C_{t-1} + b_d)$$

$$C^L_{t-1} = C_{t-1} - C^S t\text{-}1$$

$$C^{DS}_{t-1} = C^S_{t-1} \cdot g_t$$

$$C^{DL}_{t-1} = \left(C^L_{t-1} \cdot g_t'\right)$$

$$C^*_{t-1} = C^{DL}_{t-1} + C^{DS}_{t-1}$$

where W_d and b_d are the learnable parameters.

Application of egT-LSTM in Myopia Prediction

The input of each cell of egT-LSTM consists of 4 components: clinical feature x_t, elapsed time Δ_t since last time step, and elapsed time $\Delta_{t'}$ since the last measured values. The output is the current state h_t. In the myopia prediction model introduced

Table 2. The MAE of SE in the

Prediction Duration (yrs)	The MAE of SE for Different Sequence Lengths (Mean ± Standard Deviation [Sample Size]) (D)				
	1	*2*	*3*	*4*	*5*
0.25	0.26 ± 0.16 (13)*	0.05 ± 0.05 (9)*	0.02 ± 0.02 (4)*	0.01 ± 0.00 (1)*	
0.5	0.12 ± 0.13 (268)	0.09 ± 0.07 (886)	0.03 ± 0.04 (113)	0.03 ± 0.04 (92)	
0.75	0.10 ± 0.13 (839)	0.06 ± 0.06 (1404)	0.06 ± 0.06 (452)	0.06 ± 0.07 (196)	0.03 ± 0.01 (2)*
1	0.14 ± 0.15 (546)	0.08 ± 0.07 (1092)	0.06 ± 0.07 (1202)	0.06 ± 0.06 (465)	0.05 ± 0.06 (52)
1.5	0.15 ± 0.16 (302)	0.09 ± 0.10 (796)	0.05 ± 0.08 (515)	0.06 ± 0.07 (520)	0.06 ± 0.08 (78)
2	0.15 ± 0.16 (210)	0.11 ± 0.11 (432)	0.09 ± 0.1 (369)	0.065 ± 0.082 (211)	0.04 ± 0.04 (135)
3	0.18 ± 0.21 (130)	0.13 ± 0.15 (314)	0.10 ± 0.11 (248)	0.10 ± 0.11 (115)	0.07 ± 0.10 (307)
4	0.20 ± 0.20 (115)	0.16 ± 0.20 (228)	0.13 ± 0.15 (169)	0.14 ± 0.15 (92)	0.12 ± 0.16 (285)
5	0.29 ± 0.27 (205)	0.21 ± 0.18 (140)	0.13 ± 0.15 (160)	0.13 ± 0.15 (105)	0.12 ± 0.18 (69)
6	0.34 ± 0.31 (203)	0.25 ± 0.20 (85)	0.19 ± 0.22 (93)	0.19 ± 0.20 (95)	0.15 ± 0.20 (81)
7	0.45 ± 0.24 (81)	0.30 ± 0.23 (60)	0.20 ± 0.21 (72)	0.18 ± 0.18 (90)	0.15 ± 0.16 (59)
Summary	0.17 ± 0.23 (2912)	0.09 ± 0.15 (5446)	0.08 ± 0.12 (3397)	0.07 ± 0.1 (1982)	0.09 ± 0.09 (1068)

D = diopters; egT-LSTM = extended gate time-aware long short-term memory; MAE = mean absolute error; SE = spherical equivalent.
*Represents that the sample size is too small (<50) to be a solid reference.

in this paper, we incorporate 2 time-aware gates, modifying the input of each cell to include information about both time intervals. The time-aware gate for long-term memory operates as a time decay function, modifying the long-term memory based on the duration since the last measurement of the respective clinical parameter, $\Delta_{t'}$. The short-term time-aware gate, which is the second time gate, operates as a time decay function for adapting short-term memory. It calculates the elapsed time since the previous time step, Δ_t. Both the long and short time-aware gates regulate the flow of prior short or long-term memories into the present memory. The inputs fall into 2 categories, records and time intervals. An individual's record is represented by an n × 16 matrix, encompassing n instances. Within each instance, there are 16 distinct features. Correspondingly, the time intervals for each individual are represented as a vector containing n time interval values. The last time interval value aligns with the prediction duration. The resultant output corresponds to the subsequent state h_{t+1}. Ultimately, the last-step prediction involves passing this output through a fully connected neural network. The model's architecture is illustrated in Figure 3.

In the context of myopia prediction, modifying the value of the last time interval facilitates the prediction of SE values at future instances. The training parameters of the model are as follows: Learning Rate = 0.001, Batch Size = 256, Optimizer is Adam Optimizer, Epochs = 500, RNN Layers = 1, T-LSTM Hidden Size = 1024, and Early Stopping Patience = 10.

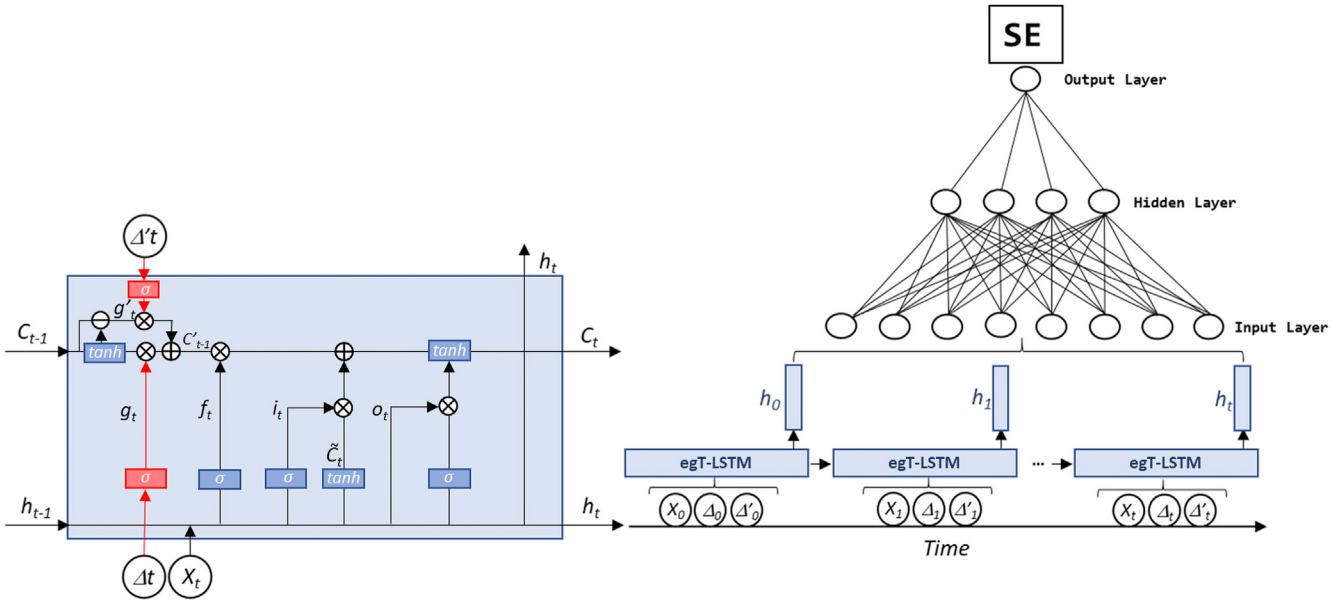

Figure 3. The architecture of egT-LSTM cell (left); red represents the unique gates in egT-LSTM and blue represents the original gates in LSTM. The prediction layers (right) combine all the hidden states learned from egT-LSTM and the static features, such as patient demographics, for the final prediction. egT-LSTM = extended gate time-aware long short-term memory; LSTM = long short-term memory; SE = spherical equivalent.

Testing Set for egT-LSTM

The MAE of SE for Different Sequence Lengths (Mean ± Standard Deviation [Sample Size]) (D)				Summary
6	7	8	9	
				0.15 ± 0.18 (27)*
				0.08 ± 0.12 (1359)
				0.07 ± 0.08 (2893)
0.02 ± 0.011 (4)*				0.08 ± 0.08 (3361)
0.06 ± 0.06 (18)*				0.08 ± 0.10 (2229)
0.04 ± 0.07 (64)	0.03 ± 0.06 (11)*			0.09 ± 0.12 (1432)
0.06 ± 0.07 (84)	0.05 ± 0.08 (23)*			0.10 ± 0.14 (1221)
0.10 ± 0.14 (168)	0.11 ± 0.12 (52)			0.13 ± 0.15 (1109)
0.11 ± 0.16 (105)	0.14 ± 0.14 (63)	0.15 ± 0.02 (3)*		0.18 ± 0.21 (853)
0.15 ± 0.18 (63)	0.14 ± 0.14 (55)	0.15 ± 0.16 (57)	0.11 ± 0.06 (5)*	0.22 ± 0.22 (737)
0.15 ± 0.15 (12)*	0.14 ± 0.14 (11)*	0.12 ± 0.10 (8)*	0.11 ± 0.12 (9)*	0.24 ± 0.24 (402)
0.09 ± 0.12 (518)	0.11 ± 0.13 (215)	0.15 ± 0.14 (71)	0.11 ± 0.11 (14)*	0.10 ± 0.15 (15623)

Metrics

The model's prediction performance is assessed using the mean absolute error (MAE), calculated as the average of the absolute deviations, as:[35]

$$MAE = \frac{1}{m}\sum_{i=1}^{m}|(yi - \acute{y}_i)|$$

It takes values in the range of $[0,+\infty)$. A smaller MAE suggests a more accurate model.

Statistical Analysis

Analysis of variance was utilized to compare means among distinct age and myopia groups, as well as to evaluate disparities in performance across various models. Data processing and statistical analyses were performed in R software (version 4.0.3, https://www.r-project.org/) and Python 3.7 (Python Software Foundation, http://www.python.org).

Ethics Declarations

The experimental protocol was established according to the ethical guidelines of the Declaration of Helsinki and was approved by the ethics committee of University Hospital "Sveti Duh," Zagreb, Croatia and the School of Medicine of the University of Zagreb, Croatia. Given the retrospective nature of the study, informed consent was not required.

Results

The cleaned dataset contains 10 170 eyes (samples) of 895 children and adolescents. Each sample is associated with 2 to 10 records. The number of samples with 2, 3, 4, 5, 6, 7, 8, 9, and 10 records is 208, 210, 216, 250, 228, 196, 210, 130, and 142, respectively. The time span between the first and last record for any given sample ranged from 0.25 years ($\leq$0.25 years) to 7 years (>6 years, <8 years). After data preprocessing, the dataset comprises an increased number of samples, reaching a total of 156 230. Sample sizes for 1, 2 ,3, 4, 5, 6, 7, 8, and 9 sequence lengths were as follows: 23 296, 43 571, 27 179, 15 859, 8546, 4141, 1720, 558, and 114, respectively.

The MAE of future SE was 0.10 ± 0.15 D on the testing set. Stratified MAE is shown in Table 2. Overall best prediction was achieved when prediction is accomplished with 4 sequence lengths, where average MAE was 0.07 ± 0.01 D, ranging from 0.03 ± 0.04 D for 0.5 years of prediction to 0.18 ± 0.18 D for a 7 years prediction. Lowest prediction was achieved with just 1 sequence length, ranging from 0.10 ± 0.13 D for 0.75 years to 0.45 ± 0.24 D for 7 years prediction duration. Regarding 4 to 6, 7 to 9, 10 to 12, 13 to 15, and 15 to 18 age groups, average MAE and standard deviations were 0.12 ± 0.12 D, 0.1 ± 0.13 D, 0.08 ± 0.11 D, 0.08 ± 0.13 D, and 0.05 ± 0.08 D ($P < 0.001$), respectively. Based on the classification of myopia, MAE and standard deviations for premyopia, low myopia, and high myopia were 0.14 ± 0.15 D, 0.10 ± 0.14 D, and 0.16 ± 0.17 D ($P < 0.001$), respectively. Illustrative examples are provided for 4 cases, Figure 4. In general, when the sequence is lengthened and the prediction time is shortened, the prediction error tends to decrease. An MAE of <0.75 D in the context of SE is considered as a prediction that meets clinical acceptability standards.[35,36]

Comparing egT-LSTM with models that can capture temporal tendency, T-LSTM and LSTM, it has been affirmed that egT-LSTM has overall best prediction performance, Table 3. Given that LSTM does not inherently handle time intervals, we treat the time intervals as an extra feature incorporated into the input records. Consequently, the input record for an individual in these models is represented as an n × 17 matrix. An example of using egT-LSTM and T-LSTM with the same record set is shown in Figure 5. The reason why egT-LSTM and T-LSTM outperform LSTM is that the preceding models can effectively capture temporal trends by individually processing temporal features, and additionally egT-LSTM compared with T-LSTM, additionally modifying the long-term memory based on the duration since the last measurement of the respective clinical parameter reduces the

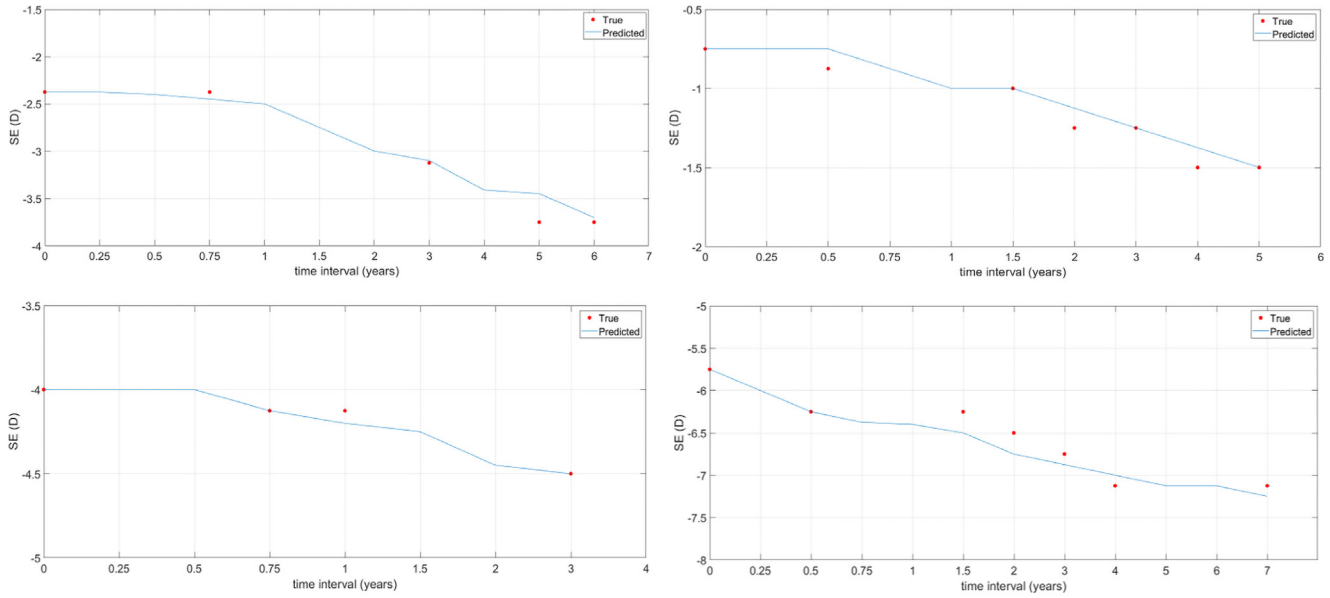

Figure 4. Four case examples of SE prediction using egT-LSTM. In each example, the curve except the starting point means the predicted value, and the red data points denote the true values. The demographic and refractive characteristics of the 4 cases were consistent with the most prevalent characteristics observed within the study sample, excluding the baseline SE. These factors included the baseline age group of 10 to 12 years, female gender, initial prescription of spectacle correction during the first visit, and the specific profile of low myopic individuals with nonmyopic parents. D = diopter; egT-LSTM = extended gate time-aware long short-term memory; SE = spherical equivalent.

impact of sparse records on trend fluctuations, lowering MAE, respectively.

Discussion

To the best of our knowledge, this is the first study achieving quantitative prediction of SE as far as 7 years in the future utilizing RNN models. Additionally, this is the first study on a European population that quantitatively predicts future SE.

Scarce data exist on quantitative predictions of future SE. Only 2 studies conducted in children and adolescents in China have achieved corresponding predictions. Lin et al,[35] engaging random forest algorithm, successfully predicted future SE quantitatively in a study involving almost 130 000 individuals in Guangdong, China, 2018. The MAE for SE prediction over 1 to 8 years ranged from 0.25 to 0.80 D. Quantitative SE prediction implementing RNN was first described by Huang et al.[37] Processing data from 37 586 children and adolescents aged 6 to 20 years in Chengdu, China, it achieved prediction within 2 and a half years. The MAE on the testing set was 0.10 ± 0.14 D, ranging from 0.04 ± 0.05 D to 0.19 ± 0.17 D considering varying historical record lengths and prediction durations. Comparing different models, RNN achieved lower MAE in comparison to random forest algorithm due to irregular time interval distribution and variable record lengths that challenge for effectively utilizing temporal information with traditional methods.[37] Implementing T-LSTM enables adept handling of data sequences with differing lengths. It excels in capturing temporal patterns by processing temporal features separately, even in cases of irregular time intervals. Taking advantage of separate processing of irregular temporal features, this paper enforced egT-LSTM, with an

Table 3. Comparison of the MAEs of Different Models

Model	The MAE of SE for Different Sequence Lengths (Mean ± Standard Deviation) (D)									Summary
	1	*2*	*3*	*4*	*5*	*6*	*7*	*8*	*9*	
egT-LSTM	0.17 ± 0.23	0.09 ± 0.15	0.08 ± 0.12	0.07 ± 0.10	0.09 ± 0.09	0.09 ± 0.12	0.11 ± 0.13	0.15 ± 0.14	0.11 ± 0.11	0.10 ± 0.15
T-LSTM	0.19 ± 0.25	0.10 ± 0.16	0.08 ± 0.13	0.08 ± 0.10	0.10 ± 0.10	0.11 ± 0.13	0.13 ± 0.13	0.16 ± 0.16	0.12 ± 0.11	0.11 ± 0.16
LSTM	0.21 ± 0.28	0.13 ± 0.16	0.08 ± 0.14	0.09 ± 0.11	0.11 ± 0.11	0.12 ± 0.13	0.14 ± 0.14	0.18 ± 0.17	0.13 ± 0.18	0.13 ± 0.17
P-value	**< 0.001**	**< 0.001**	**< 0.001**	**< 0.001**	**< 0.001**	**< 0.001**	**0.01**	**0.04**	0.12	**< 0.001**

ANOVA was used to test the significance of difference between groups.
Bolded values represent statistically significant values.
ANOVA = analysis of variance; D = diopters; egT-LSTM = extended gate time-aware long short-term memory; LSTM = long short-term memory; MAE = mean absolute error; SE = spherical equivalent; T-LSTM = time-aware long short-term memory.

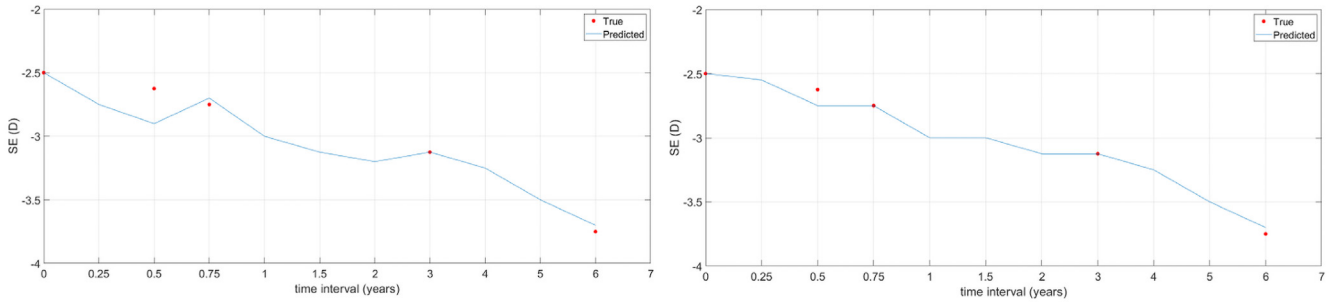

Figure 5. A case example of SE prediction using T-LSTM, left figure, and egT-LSTM, right figure. In each example, the curve except the starting point means the predicted value, and the red data points denote the true value. Based on the initial parameters that suggested potential rapid myopia progression (both parents myopic, a preschool-aged female child, aged 6−7 years) and with incomplete follow-up data and irregular attendance at scheduled follow-ups, this case exemplifies how the egT-LSTM model can provide more stable predictions of SE in asynchronous and sparse records, compared with the T-LSTM model. D = diopters; egT-LSTM = extended gate time-aware long short-term memory; SE = spherical equivalent; T-LSTM = time-aware long short-term memory.

additional time-aware trait. Gathering extensive, reliable fact-based clinical data on a large scale is a time-consuming and gradual process.[10] As a result, best quantitative SE prediction models utilize historical demographic and refractive data. Because of consistently linked sparse records and varying time intervals between measurements, we proposed adjustment of short-term memory to not only time intervals between variable streams, but also the elapsed time since the last measured values for each variable stream. Comparing T-LSTM and egT-LSTM on similar patient records, less fluctuations and lower MAE was obtained using egT-LSTM, Figure 5.

The meaningfulness of a prediction is contingent upon its precision and timely arrival, granting an extra clinical advantage. As demonstrated by our results, egT-LSTM achieves a clinically acceptable prediction[35,36] as far as 7 years in the future. Despite statistically significant differences in MAE across various age or myopia classification groups, these differences fall below the threshold of objective refraction measurement error at group levels.[38] Thus, from a clinical perspective, these variations are insignificant. It is important to note the substantial variability observed in objective refraction measurement error at the individual level.[38] This underscores the crucial need for precise "long-term" predictions that are of utmost importance, especially considering the potential side effects of current myopia control treatments, which, while effective, require careful and effective utilization.[5,39] Moreover, early and accurate prediction of myopia during its initial stages is crucial to optimize the benefits of treatment. At the moment, using TensorBoard, a software named MyopiaMomentum is under development. Based on the initial examination variables, the model would generate numerical and graphical predictions of myopia progression.

The current study has some limitations. Firstly, the number of myopic individuals in the Republic of Croatia is significantly lower than in Asian countries. However, the long follow-up period and inclusion of just primary myopic individuals enabled high sample numbers after data preprocessing. Secondly, implementation of ocular biometric data could improve accuracy of egT-LSTM even more; however, our model achieved similar prediction accuracy[36] even without axial length measurements and corneal curvature, which is in concordance to other recent studies on myopia prediction.[40] Thirdly, myopia progression is related to many other factors like time spent outdoors, near work activity time, digital screen time, and degree of room illumination.[41] Nonetheless, our dataset is limited to visual screening records and parental myopia data, as other environmental data records were not accessible for this study. Utilizing multimodal learning, which incorporates vision records and various quantitative environmental data, could enhance prediction accuracy even further.

Our study introduced a novel approach using egT-LSTM to accurately forecast SE progression in myopic children and adolescents over a 7-year span. By precisely predicting SE evolution, the model enables early detection of myopia progression, facilitating timely interventions crucial for effective myopia prevention and management strategies. This innovative use of egT-LSTM underscores deep learning's ability to capture intricate temporal patterns in irregularly sampled time series data, aligning more closely with fact-based data characteristics and thereby enhancing its applicability. These advancements offer promising avenues for further refinement in myopia prediction and control strategies. Furthermore, acknowledging serious repercussions of untreated myopia underscores the importance of our quantitative SE prediction model in assisting individuals at risk of rapid progression and enabling targeted interventions. This substantially contributes to the overarching objective of myopia prevention and control. The adoption of egT-LSTM represents a substantial leap forward, enabling the extraction of temporal features from complex datasets and thereby improving the applicability and precision of myopia prediction models amidst the intricate nature of myopia progression.

Footnotes and Disclosures

Originally received: February 25, 2024.
Final revision: May 26, 2024.
Accepted: June 5, 2024.
Available online June 13, 2024. Manuscript no. XOPS-D-24-00062.

[1] University Eye Department, University Hospital "Sveti Duh", Reference Center of The Ministry of Health of The Republic of Croatia for Pediatric Ophthalmology and Strabismus, Reference Center of The Ministry of Health of The Republic of Croatia for Inherited Retinal Dystrophies, Zagreb, Croatia.

[2] Faculty of Dental Medicine and Health Osijek, University Josip Juraj Strossmayer in Osijek, Croatia.

[3] Department of Medical Statistics, Epidemiology and Medical Informatics, Andrija Štampar School of Public Health, School of Medicine, University of Zagreb, Zagreb, Croatia.

Disclosure(s):

All authors have completed and submitted the ICMJE disclosures form.

The authors have no proprietary or commercial interest in any materials discussed in this article.

HUMAN SUBJECTS: Human subjects were included in this study. The experimental protocol was established according to the ethical guidelines of the Declaration of Helsinki and was approved by the ethics committee of University Hospital "Sveti Duh," Zagreb, Croatia and the School of Medicine of the University of Zagreb, Croatia. Given the retrospective nature of the study, informed consent was not required.

No animal subjects were included in this study.

Author Contributions:

Conception and design: Varošanec, Marković, Sonicki

Data collection: Varošanec, Marković

Analysis and interpretation: Varošanec, Marković, Sonicki

Obtained funding: Study was performed as part of the PhD study from Ana Maria Varošanec. No additional funding was provided.

Overall responsibility: Varošanec, Marković, Sonicki

American Academy of Ophthalmology Annual Meeting, 2023, San Francisco Nov. 3-6, poster presentation titled: Myopia Prediction for Children and Adolescents of Central and Southeast Europe Using Advanced Machine Learning Methods; Ana Maria Varosanec, MD; Zdenko Sonicki, MD; Mirjana Bjelos, MD; Mladen Busic, MD; Leon Markovic, MD.

Abbreviations and Acronyms:
D = diopters; **egT-LSTM** = extended gate time-aware long short-term memory; **LSTM** = long short-term memory; **MAE** = mean absolute error; **RNN** = recurrent neural network; **SE** = spherical equivalent; **T-LSTM** = time-aware long short-term memory.

Keywords:
Deep learning, Myopia, Spherical equivalent refraction.

Correspondence:
Leon Marković, MD, University Eye Department, University Hospital "Sveti Duh", Reference Center of the Ministry of Health of the Republic of Croatia for Pediatric Ophthalmology and Strabismus, Reference Center of the Ministry of Health of the Republic of Croatia for Inherited Retinal Dystrophies, 10000 Zagreb, Croatia; Faculty of Dental Medicine and Health Osijek, University Josip Juraj Strossmayer in Osijek, 31000 Osijek, Croatia. E-mail: lemarkovic@gmail.com.

References

1. Holden BA, Fricke TR, Wilson DA, et al. Global prevalence of myopia and high myopia and temporal trends from 2000 through 2050. *Ophthalmology*. 2016;123(5):1036−1042.
2. Cooper J, Tkatchenko AV. A review of current concepts of the etiology and treatment of myopia. *Eye Contact Lens*. 2018;44(4):231−247.
3. Baird PN, Saw SM, Lanca C, et al. Myopia. *Nat Rev Dis Prim*. 2020;6(1):99.
4. Wildsoet CF, Chia A, Cho P, et al. Imi - interventions myopia institute: interventions for controlling myopia onset and progression report [published correction appears in Invest Ophthalmol Vis Sci. 2019 Apr 1;60(5):1768] *Invest Ophthalmol Vis Sci*. 2019;60(3):M106−M131.
5. Zhang XJ, Zhang Y, Yip BHK, et al. Five-year clinical trial of low-concentration atropine for myopia progression (LAMP) study: phase 4 report. *Ophthalmology*. 2024.
6. Han X, Liu C, Chen Y, He M. Myopia prediction: a systematic review. *Eye*. 2022;36(5):921−929.
7. French AN, Morgan IG, Mitchell P, Rose KA. Risk factors for incident myopia in Australian schoolchildren: the Sydney adolescent vascular and eye study. *Ophthalmology*. 2013;120(10):2100−2108.
8. Fan Q, Guo X, Tideman JW, et al. Childhood gene-environment interactions and age-dependent effects of genetic variants associated with refractive error and myopia: the CREAM Consortium. *Sci Rep*. 2016;6:25853.
9. Tedja MS, Haarman AEG, Meester-Smoor MA, et al. Imi - myopia genetics report. *Invest Ophthalmol Vis Sci*. 2019;60(3):M89−M105.
10. Matsumura S, Lanca C, Htoon HM, et al. Annual myopia progression and subsequent 2-year myopia progression in Singaporean children. *Transl Vis Sci Technol*. 2020;9(13):12.
11. Lee CKM, Yi Cao. Big data analytics for predictive maintenance strategies, In: Supply Chain Management in the Big Data Era. *IGI Global*. 2016:50−74.
12. Deo RC. Machine learning in medicine. *Circulation*. 2015;132(20):1920−1930.
13. Jiang Y, Yang M, Wang S, et al. Emerging role of deep learning-based artificial intelligence in tumor pathology. *Cancer Commun*. 2020;40(4):154−166.
14. Li Z, Zhou L, Bin X, et al. Utility of deep learning for the diagnosis of cochlear malformation on temporal bone CT. *Jpn J Radiol*. 2024;42(3):261−267.
15. Lu J, Tong X, Wu H, et al. Image classification and auxiliary diagnosis system for hyperpigmented skin diseases based on deep learning. *Heliyon*. 2023;9(9):e20186.
16. Liu LJ, Ortiz-Soriano V, Neyra JA, Chen J. KIT-LSTM: knowledge-guided time-aware LSTM for continuous clinical risk prediction. *Proceedings (IEEE Int Conf Bioinformatics Biomed)*. 2022;2022:1086−1091.
17. Flitcroft DI, He M, Jonas JB, et al. Imi - defining and classifying myopia: a proposed set of standards for clinical and epidemiologic studies. *Invest Ophthalmol Vis Sci*. 2019;60(3):M20−M30.
18. Sree KPNVS, Niharika C, Ravinder N, et al. Optimized conversion of categorical and numerical features in machine learning models. In: *2021 Fifth International Conference on I-SMAC (IoT in Social, Mobile, Analytics and Cloud)*. I-SMAC; 2021:294−299.

19. Sharma P, Singh J. Machine learning based effort estimation using standardization. In: *2018 International Conference on Computing, Power and Communication Technologies (GUCON), Greater Noida, India*. 2018:716−720.
20. Pascanu R, Mikolov T, Bengio Y. On the difficulty of training recurrent neural networks. In: *Proceedings of the 30th International Conference on Machine Learning, Atlanta, Georgia, USA*. 28. 2013:1310−1318.
21. Zaremba W, Sutskever I, Vinyals O. Recurrent neural network regularization. *arXiv*. 2014. https://doi.org/10.48550/arXiv.1409.2329.
22. Hochreiter S, Schmidhuber J. Long short-term memory. *Neural Comput*. 1997;9(8):1735−1780.
23. Baytas I, Xiao C, Zhang X, et al. Patient subtyping via time-aware lstm networks. In: *Proceedings of the 23rd ACM SIGKDD international conference on knowledge discovery and data mining*. 2017:65−74.
24. Kang MW, Kim J, Kim DK, et al. Machine learning algorithm to predict mortality in patients undergoing continuous renal replacement therapy. *Crit Care*. 2020;24(1):42.
25. Rose S. Machine learning for prediction in electronic health data. *JAMA Netw Open*. 2018;1(4):e181404.
26. Neil D, Pfeiffer M, Liu S-C. Phased lstm: accelerating recurrent network training for long or event-based sequences. *arXiv*. 2016. https://doi.org/10.48550/arXiv.1610.09513.
27. Ayala Solares JR, Diletta Raimondi FE, Zhu Y, et al. Deep learning for electronic health records: a comparative review of multiple deep neural architectures. *J Biomed Inform*. 2020;101:103337.
28. W. Cao, D. Wang, J. Li, et al., Brits: bidirectional recurrent imputation for time series, *Adv Neural Inf Process Syst*, In Proceedings of the 32nd International Conference on Neural Information Processing Systems (NIPS'18). Curran Associates Inc., Red Hook, NY, USA, 6776−6786.
29. Ahmad MA, Eckert C, Teredesai A. Interpretable machine learning in healthcare. *Proceedings of the 2018 ACM international conference on bioinformatics, computational biology, and health informatics*. 2018:559−560.
30. Cheng Y, Wang F, Zhang P, Hu J. Risk prediction with electronic health records: a deep learning approach. In: *Proceedings of the 2016 SIAM International Conference on Data Mining, Miami, Florida, USA*. SIAM; 2016:432−440.
31. Shawwa K, Ghosh E, Lanius S, et al. Predicting acute kidney injury in critically ill patients using comorbid conditions utilizing machine learning. *Clin Kidney J*. 2020;14(5):1428−1435.
32. Yadav P, Steinbach M, Kumar V, Simon G. Mining electronic health records (ehrs) a survey. *ACM Comput Surv*. 2018;50(6):1−40.
33. Wu S, Liu S, Sohn S, et al. Modeling asynchronous event sequences with RNNs. *J Biomed Inform*. 2018;83:167−177.
34. Vaswani A, Shazeer N, Parmar N, et al. Attention is all you need. In: *Advances in neural information processing systems*. 2017:5998−6008.
35. Lin H, Long E, Ding X, et al. Prediction of myopia development among Chinese school-aged children using refraction data from electronic medical records: a retrospective, multicentre machine learning study. *PLoS Med*. 2018;15(11):e1002674.
36. Smith G. Refraction and visual acuity measurements: what are their measurement uncertainties? *Clin Exp Optom*. 2006;89(2):66−72.
37. Huang J, Ma W, Li R, et al. Myopia prediction for children and adolescents via time-aware deep learning. *Sci Rep*. 2023;13(1):5430.
38. Wilson LB, Melia M, Kraker RT, et al. Accuracy of autorefraction in children: a report by the American Academy of ophthalmology. *Ophthalmology*. 2020;127(9):1259−1267.
39. Hiraoka T, Kakita T, Okamoto F, et al. Long-term effect of overnight orthokeratology on axial length elongation in childhood myopia: a 5-year follow-up study. *Invest Ophthalmol Vis Sci*. 2012;53(7):3913−3919.
40. Chen Y, Tan C, Foo LL, et al. Development and validation of a model to predict who will develop myopia in the following year as a criterion to define premyopia. *Asia Pac J Ophthalmol (Phila)*. 2023;12(1):38−43.
41. Yang Z, Wang X, Zhang S, et al. Pediatric myopia progression during the COVID-19 pandemic home quarantine and the risk factors: a systematic review and meta-analysis. *Front Public Health*. 2022;10:835449.